Synthesis and Biological Evaluation of Colchicine B-Ring Analogues Tethered with Halogenated Benzyl Moieties

Laura Cosentino,[†,⊥] Mariano Redondo-Horcajo,[‖] Ying Zhao,[§] Ana Rita Santos,[†] Kaniz F. Chowdury,[†] Victoria Vinader,[†] Qasem M. A. Abdallah,[†,#] Hamdy Abdel-Rahman,[†,∞] Jérémie Fournier-Dit-Chabert,[†] Steven D. Shnyder,[†] Paul M. Loadman,[†] Wei-shuo Fang,[§] José Fernando Díaz,[‖] Isabel Barasoain,[‖] Philip A. Burns,[‡] and Klaus Pors*,[†]

[†]Institute of Cancer Therapeutics, University of Bradford, Bradford, West Yorkshire, BD7 1DP, U.K.

[‡]Section of Pathology and Tumor Biology, Leeds Institute of Molecular Medicine, St. James's University Hospital, Leeds, LS9 7TF, U.K.

[§]Institute of Materia Medica, Chinese Academy of Medical Sciences and Peking Union Medical College, 1 Xian Nong Tan Street, Beijing 100050, P. R. China

[‖]Centro de Investigaciones Biológicas, CSIC, 28040, Madrid, Spain

Ⓢ Supporting Information

ABSTRACT: Deacetylcolchicine was reacted with substituted benzyl halides to provide a library of compounds for biological analysis. Compound 7 (3,4-difluorobenzyl-N-aminocolchicine) was shown to possess cytotoxicity in cancer cell lines in the low nanomolar range. Significantly, it showed no loss of activity in the resistant A2780AD ovarian carcinoma cell line known to overexpress the ABCB1 drug transporter and was also unaffected by overexpression of class III β-tubulin in HeLa transfected cells.

INTRODUCTION

Although microtubule disrupting agents are among the most successful drugs used in chemotherapy, they are often ineffective against cancer cells displaying multidrug-resistance (MDR).[1] Central to MDR is the membrane-bound P-glycoprotein (P-gp, ABCB1, MDR1), which is overexpressed in several different tumor types and known to be associated with poor response to chemotherapy.[2] Resistance to different classes of microtubule disrupting agents may also be tumor specific. For example, the *Vinca* alkaloids are mostly effective against hematological cancers but often ineffective against solid tumors and taxoids such as paclitaxel and are effective in treating ovarian, mammary, and lung tumors but not other solid tumors such as colon carcinomas.[3] Colchicine, the main alkaloid of the poisonous plant meadow saffron (*Colchicum autumnale* L.), is used for the treatment of gout and familial Mediterranean fever.[4] Although colchicine is not clinically used to treat cancer because of toxicity, it exerts antiproliferative effects through the inhibition of microtubule formation, leading to mitotic arrest, antivascular disruption, and cell death by apoptosis.[5] It is well-established that synthetic modifications to the A-ring are associated with loss of biological activity while there is some tolerance in regard to manipulation of the C-ring.[6] In contrast, modification of the B-ring at the terminal acetamide has led to interesting accounts detailing structure–activity relationships (SARs), some aimed at overcoming MDR in cancer,[7−9] while others including ourselves have investigated ways of delivering high doses to tumor tissue while not affecting normal tissue.[10] Significantly, we have shown that agents with capacity to covalently bind microtubules possess properties that are essential in overcoming MDR.[11,12] Similarly, it can be hypothesized that compounds with increased affinity for

the colchicine binding domain will lead to improved therapeutic index by increasing selectivity for the cellular target, reducing availability for drug efflux via P-gp and leading to an overall reduction in toxicity. As an extension of our ongoing efforts to develop novel analogues that evade traditional resistance mechanisms and possess improved target selectivity, we here report on a library of compounds derived from colchicine, which have been modified to improve the affinity at the colchicine binding domain.

RESULTS AND DISCUSSION

Chemistry. The synthetic route to the novel compounds encompassed traditional synthetic modifications. The C7 acetamide group at the B-ring was removed in a three-step procedure as previously reported.[13] Deacetylcolchicine was reacted with substituted benzyl bromides to afford target compounds with 40−71% yields (Scheme 1).

Computational Chemistry. The X-ray crystal structure of bovine α,β-tubulin complexed with N-deacetyl-N-(2-mercaptoacetyl)colchicine was obtained from the protein database (PDB code 1SA0, 3.58 Å) as previously described.[14] MOE software was employed to generate binding models for 1−11, which were energy-minimized prior to calculating their binding affinities. The incorporation of the benzyl fragments at the deacetylcolchicine B-ring position led to at least 1 order of magnitude higher affinity in all compounds for the colchicine tubulin binding site (Table 1). All the colchicine models revealed

Scheme 1. Synthetic Route to Colchicine B-Modified Analogues

Figure 1. Compound **7** docked into the colchicine binding site.
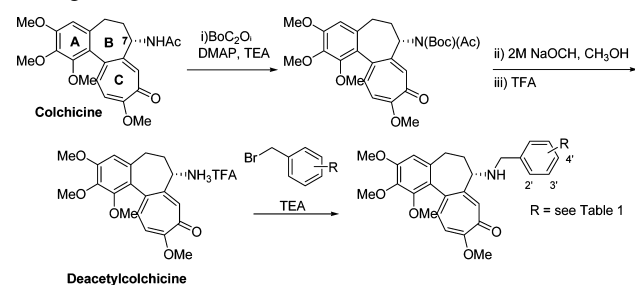
how the benzyl fragment occupied the chemical space available in the binding pocket more efficiently than the acetamide group of colchicine (Figures S1−S11). A previous study focused on isocolchicine derivatives demonstrated that these were able to interact with α-tubulin through B-ring substitution in the colchicine scaffold, thereby increasing their overall binding affinity for the protein.[15] As an example of the binding of the benzyl tethered colchicines in this study, Figure 1 shows **7** docked into the colchicine binding site, revealing the 3′,4′-difluorobenzyl moiety to be well accommodated.

Inhibition of Tubulin Assembly. The colchicinoids were incubated with purified bovine brain tubulin and investigated for the ability to inhibit tubulin polymerization using conditions previously described.[16] From the data in Table 1, the new analogues exhibited strong inhibition of tubulin assembly with **5**−**7** approximately 5 times more potent than colchicine.

Chemosensitivity. The modified colchicines were evaluated for their ability to inhibit the growth of DLD-1 colorectal cancer cells. All compounds, bar **10** which precipitated out, displayed potent cytotoxicity in the low 1−50 nM range. Although data from computational modeling and the microtubule polymerization assay demonstrated all new compounds to be more affinic for the colchicine binding site than colchicine, only **6** (3-fold) and **7** (10-fold) were actually more cytotoxic with **4** and **11** being equicytotoxic. To obtain further SAR information, we evaluated the fluorinated compounds within this series (**5**−**9**) and the 4′-OCH₃ (**11**) analogue in the HT29 colon cancer cell line, and the more aggressive MDA-MB-231 breast cancer cell line. Generally, the compounds were found to possess similar potency in the HT29 cells as was observed for the DLD-1 cells, but all
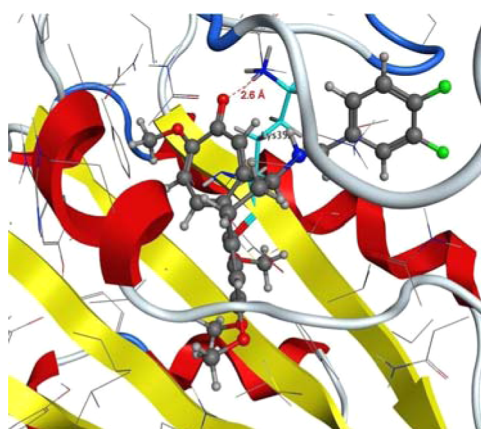
compounds including colchicine lost 3- to 20-fold potency in the MDA-MB-231 cells. Within the fluorine series it was apparent that the monosubstituted **5** or compounds containing fluorine in the 5′-position of the attached benzyl moiety (**8** and **9**) lost potency compared to 2′,3′- (**6**) or 3′,4′- (**7**) disubstituted analogues, which is noteworthy given that the computational modeling did not predict these empirical data. Compound **7** was shown to be consistently more potent than colchicine, exhibiting low nanomolar cytotoxicity (1−15 nM) across the three cancer cell lines investigated; hence, it was selected for further studies.

Cell Cycle and Microtubule Disruption. Exposure of HT29 cells to **7** led to accumulation of cells in the late G2/M phase after 24 h (92.5%) or 48 h (91.2%), which was not observed for untreated control samples (12.7% and 8.8%, respectively), revealing similar cell cycle profile to colchicine but with a more potent agent (Figure S12). To evaluate the effect on endothelial cell morphology and cytoskeletal organization, HT29 cells were exposed to **7** for 24 h followed by tubulin immunostaining. Analysis of the results revealed changes to the cell shape and disruption of the microtubule network in a dose-dependent manner (Figure 2).

Drug Resistance. Although **7** is more potent than colchicine across the three cancer cell lines, the mechanism for this biological activity appeared to be similar, given the experimental observations from the cell cycle and morphological studies. Indeed, the increased activity could be associated with higher

Table 1. Physicochemical Properties, Tubulin Binding Affinities, and Growth Inhibition against a Human Cancer Cell Lines

compd	R	MW	CLogP[a]	affinity [pKᵢ][b]	ITA[c] IC₅₀ [μM]	DLD-1[d] IC₅₀ [nM]	HT-29 IC₅₀ [nM]	MDA-MB-231 IC₅₀ [nM]
colchicine	H	399.4	2.586	8.792	7.85 ± 0.89	15.6 ± 0.46	69.25 ± 6.71	37 ± 1.41
1	4′-Br	447.5	4.506	9.435	ND[e]	31.17 ± 1.26	ND[e]	ND[e]
2	4′-Cl	526.4	5.269	9.897	1.70 ± 0.20	32.60 ± 0.66	ND[e]	ND[e]
3	4′-I	465.2	4.645	9.553	ND[e]	35.90 ± 1.10	ND[e]	ND[e]
4	4′-F	482.0	5.160	9.737	ND[e]	11.38 ± 0.41	ND[e]	ND[e]
5	3′-F	573.4	5.111	9.914	1.49 ± 0.18	51.6 ± 5.33	63.4 ± 2.3	89.1 ± 1.3
6	2′,3′-F	483.5	4.784	9.703	1.62 ± 0.15	4.67 ± 0.15	7.43 ± 5.73	86 ± 3.47
7	3′,4′-F	483.5	4.784	9.846	1.52 ± 0.18	1.61 ± 0.13	4.3 ± 1.14	16 ± 2.22
8	3′,5′-F	483.5	4.784	9.882	2.98 ± 0.29	35.2 ± 0.80	52 ± 1.2	523 ± 5.34
9	3′,4′,5′-F	501.5	4.923	10.196	4.60 ± 0.42	36.2 ± 0.25	64.5 ± 1.03	92.2 ± 1.95
10	4′-NO₂	492.5	4.414	10.233	1.99 ± 0.21	Prec[f]	ND[e]	ND[e]
11	4′-OCH₃	477.6	4.515	10.337	6.49 ± 0.68	15.7 ± 0.59	51 ± 3.13	93 ± 6.06

[a]CLogP was calculated using the Wildman and Crippen model. [b]The calculated binding affinity was generated using MOE software. [c]Inhibition of tubulin assembly (IC₅₀ = concentration required to inhibit 50% of the DAPI-fluorescence enhancement due to tubulin polymerization). [d]IC₅₀ values are the mean ± SD of at least three independent assays. [e]ND = not determined. [f]Prec = compound precipitation, no IC₅₀.
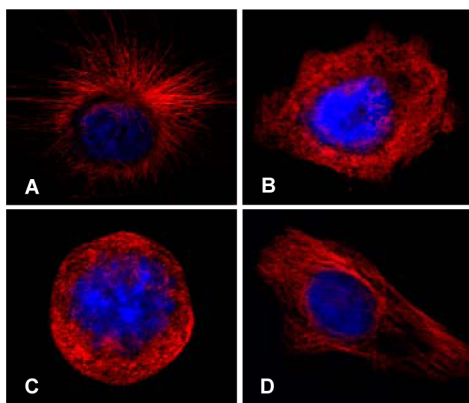
Figure 2. Disruption of the microtubules. HT29 cells were exposed to **7** at 5 (A), 50 (B), and 500 nM (C) for 24 h and compared to untreated cells (D). Microtubules are stained in red. Chromatin is in blue.

lipophilicity and more efficient cellular uptake of **7** ($\log P = 4.78$) compared with colchicine ($\log P = 2.586$). Colchicine undergoes intensive hepatic metabolism with B-ring deacetylation through CYP3A4, and the excretion is largely dependent on P-gp.[17] Incubation of **7** with mouse liver homogenate revealed no breakdown products after 2 h, demonstrating that modification of the acetamide with a 3,4-difluorobenzyl moiety provides stability to the compound (Figure S13). Evaluation of **7** in the A2780 ovarian carcinoma cell line and the P-gp overexpressing A2780AD variant showed that this compound was unaffected by P-gp expression. In contrast, colchicine and paclitaxel lost 2.5- and 900-fold in potency, respectively (Table 2).

Table 2. Growth Inhibition of A2780 Parental and A2780AD Resistant Ovarian Carcinoma Cells by 7, Colchicine, and Paclitaxel

compd	IC$_{50}$^{a} [nM]		RF^b
	A2780	A2780AD	
7	18.8 ± 1.4	17.2 ± 1.4	0.9
colchicine	6.7 ± 0.4	16.8 ± 1.1	2.5
paclitaxel	1.1 ± 0.5^b	>1000	>900

^{a}IC$_{50}$ values are the mean $\pm$ standard error of at least four independent assays. ^{b}The resistance factor (RF) = IC$_{50}$ of the A2780AD cell line/IC$_{50}$ of the parental A2780 cell line.

Induction of ABC Transporter Proteins. In addition to using the ABCB1-overexpressing A2780AD cell line, further studies evaluated whether colchicine or the new analogue **7** would induce this transporter or ABCG2 (BCRP1). The latter is another transporter protein that has been shown to cause resistance to drugs such as camptothecin and mitoxantrone.[2] Given the lack of clinical success of taxoids in the treatment of colon carcinomas, HT29 and DLD-1 cell lines were utilized. To determine the effect on gene transcript level, cells were exposed for 96 h to concentrations equal to IC$_{50}$ or $^1/_{10}$ of the IC$_{50}$. QRT-PCR was used to quantitatively examine gene expression levels by combining with reverse transcription and measuring mRNA levels for the two ABC genes. The results shown in Figure 3 revealed that induction at the gene level is possible in the HT29 cells but not in the DLD-1 cells, suggesting that long-term exposure may lead to resistance via ABCB1 and ABCG2 in the former cell line. In contrast, the short-term chemosensitivity assays revealed that **7** was not affected by high levels of ABCB1 in
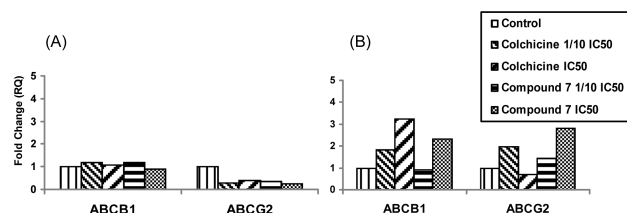
Figure 3. Effects of **7** and colchicine on the induction of ABCB1 and ABCG2 transporter genes in DLD-1 (A) and HT29 (B) cells.

the A270AD cells and it was not judged a good substrate for ABCG2 in A549 cells (known to express the highest levels of ABCG2 function among cells in the NCI 60 human cancer cell line screen[19]) given its cytotoxicity was not affected by the presence of the ABCG2 inhibitor fumitremorgin C (Figure S14).

Tubulin Resistance. A recent study[20] disclosed evidence that several agents able to bind at the colchicine site of tubulin were unaffected by class III β-tubulin resistance, indicating that new compounds affinic for this site could play a role as an alternative option to taxoids against patients that relapse because of drug-resistant tumors. In this respect, we also evaluated **7** in parental HeLa cells and a transfected β-III resistant variant.[21] The latter is resistant to agents binding at the paclitaxel binding site and the *Vinca* alkaloid binding site.[22] As the data in Table 3

Table 3. Growth Inhibition of HeLa Parental and HeLa β-III Transfected Cervix Carcinoma Cells by 7, Colchicine, and Paclitaxel

compd	IC$_{50}$^{a} [nM]		RF^b
	HeLa	HeLa βIII	
7	25.3 ± 0.8	14.1 ± 0.8	0.55
colchicine	8.2 ± 0.3	9.7 ± 0.3	1.2
paclitaxel	1.0 ± 0.1	11.2 ± 0.1	11.2

^{a}IC$_{50}$ values are the mean $\pm$ standard error of at least four independent assays. ^{b}The resistance factor (RF) = IC$_{50}$ of the resistant HeLa β-III cell line/IC$_{50}$ of the HeLa cell line.

reveal, **7** not only is equipotent in the β-III tubulin transfected cancer cell line but has an almost 2-fold increased activity. The reason for this might be that transfected HeLa cells overexpress class III β-tubulin, which may induce an increase in microtubule dynamics. This would explain why agents binding at the colchicine site are working more efficiently compared with microtubule stabilization agents such as the taxoids.

■ CONCLUSION

Despite of the emergence of molecularly targeted agents, microtubule-targeting agents will continue to offer physicians viable therapeutic options to combat cancer in the foreseeable future.[3,23] However, no compounds based on the colchicine scaffold have been successful in treating cancer patients. Many factors related to the colchicine architecture warrant further exploration including the structural simplicity of the scaffold, the availability of the natural product, the ease with which this natural product can be synthetically manipulated, the ability to down-regulate several drug-metabolizing cytochrome P450 enzymes[18] and hence avoid phase I metabolism, and ability to evade class III β-tubulin resistance. Our ongoing synthetic and biological studies on several different classes of anticancer agents are aimed at combining properties that make cytotoxics and prodrugs evade conventional resistance mechanisms but also

exploiting the tumor microenvironment to deliver sufficient doses of compound to elicit an efficient therapeutic response.[10,24,25] We have reported here a new library of colchicine analogues modified at the B-ring by incorporation of aryl-substituted fragments, typified by **7**, which in comparison with colchicine possesses improved biological activity against sensitive and resistant cancer cells in vitro. This study is important in identifying novel leads for further development of agents that can evade conventional resistance mechanisms, thereby improving on the therapeutic index of colchicine.

■ EXPERIMENTAL SECTION

All chemicals were obtained from Aldrich and Lancaster. Solvents were supplied by VWR bar anh THF (Aldrich). For column chromatography, silica particle size was $35-70$ μm. Thin layer chromatography plates (on aluminum) were supplied by VWR. ^{1}H and ^{13}C NMR spectra were measured on a Bruker Advance AM 400 (400 MHz) spectrometer, and low resolution mass spectra were generated using a Micromass Quattro Ultima mass spectrometer. The purity of all compounds was ≥95% as measured by HPLC analysis. A representative example of target compound synthesis is described below.

3,4-Difluorobenzyl-*N*-aminocolchicine (7). To a stirring solution of *N*-deacetylcolchicine (50 mg, 0.140 mmol) in anhydrous THF (3 mL) under argon atmosphere were added 3,4-difluorobenzyl bromide (43.5 mg, 0.210 mmol) and NEt$_3$ (39 μL, 0.280 mmol). The resulting solution was heated at 65 °C for 16 h. The reaction mixture was then poured in saturated NaHCO$_3$ (20 mL) and extracted with CH$_2$Cl$_2$ (3×25 mL). The combined organic extracts were dried over MgSO$_4$, and the solvent was removed under vacuum. The crude oil was subjected to column chromatography on silica gel (petroleum ether/EtOAc 1:1 → EtOAc) to give the title compound as a yellowish solid (44 mg, 65%). ^{1}H (400 MHz, CDCl$_3$): 1.61–1.74 (m, 1H, H6), 2.17–2.26 (m, 1H, H6'), 2.34–2.42 (m, 1H, H5), 2.47 (dd, 1H, *J* 6.1 and 13.6 Hz, H5'), 3.37–3.42 (m, 2H, H7 and H14), 3.57 (s, 3H, OCH$_3$), 3.68 (d, 1H, *J* 13.5 Hz, H14'), 3.90 (s, 3H, OCH$_3$), 3.90 (s, 3H, OCH$_3$), 4.00 (s, 3H, OCH$_3$), 6.52 (s, 1H, HAr), 6.81 (d, 1 H, *J* 10.7 Hz, HAr), 6.93–7.10 (m, 3 H, HAr), 7.23 (d, 2 H, *J* 10.7 HAr), 7.80 (s, 1H, HAr). ^{13}C (101 MHz, CDCl$_3$): 30.2 (C5), 38.7 (C6), 50.6 (C14), 56.0 (OCH$_3$), 56.3 (OCH$_3$), 59.9 (C7), 60.8 (OCH$_3$), 61.2 (OCH$_3$), 107.1 (CHAr), 111.9 (CHAr), 116.9 (d, *J* 9.4 Hz, CHAr), 117.0 (d, *J* 9.4 Hz, CHAr), 123.9 (dd, *J* 3.5 and 6.0 Hz, CHAr), 125.3 (CAr), 132.0 (CHAr), 134.9 (CHAr), 135.0 (CAr), 136.6 (brs CAr), 136.9 (CAr), 141.1 (CAr), 148.1 (d, *J* 12.6 Hz, CAr), 148.9 (d, *J* 12.7 Hz, CAr), 150.5 (d, *J* 12.3 Hz, CAr), 150.6 (Car,) 151.3 (d, *J* 12.5 Hz, CAr), 153.3 (CAr), 163.9 (CAr), 179.7 (CO). *m/z* (ES+) 484 [M + H]$^+$ (100%). HMRS calcd for C$_{27}$H$_{28}$O$_5$N$_1$F$_2$ 484.1930, found 484.1934 [M + H]$^+$.

Molecular Modeling. By use of the information from the X-ray structure (PDB code 1SA0), mercaptocolchicine was modified to colchicine and **1−11**, following minimization, binding energy estimates were calculated using a previously described method.[14]

Inhibition of Tubulin Assembly. Tubulin containing microtubule-associated protein (MAP) was isolated from pig brain by assembly/disassembly cycles.[26] Compounds were evaluated for inhibition of the polymerization of MAP-tubulin with minor modification to previous protocol.[16] Briefly, reaction mixtures containing PMEG buffer (0.1 M PIPES, 1 mM MgSO$_4$, 2 mM EGTA, 10% glycerol, 0.1 mM GTP, pH 6.9), 10 μM MAP-tubulin, and 10 μM DAPI were prepared at 0 °C and 200 μL was added per well in a 96-well plate. Compounds were added at appropriate concentrations (0.2–50 μM). Fluorescence data were collected using TECAN Infinite F200 plate reader (excitation 360/35, emission 465/35) at 37 °C for 60 at 1 min intervals. The IC$_{50}$ was obtained by the software GraphPad Prism 4.00 using the following nonlinear regression fitting equation: $\Delta F = \Delta F_{max}[\text{drug}]/(\text{IC}_{50} + [\text{drug}])$. At least three independent determinations were performed for each compound.

Chemosensitivity. The cell lines DLD-1, HT29, and MBD-DA-431 were cultured in RPMI 1640 cell culture medium supplemented with 1 mM sodium pyruvate, 2 mM L-glutamine, and 10% fetal bovine serum

(all from Sigma). A2780 and A2780AD ovary carcinoma cell lines were supplemented as well with 0.25 units/mL bovine insulin. HeLa and HeLa β-III[21] cervix carcinoma lines were grown in DMEM supplemented with sodium pyruvate, glutamine, and fetal bovine serum as above, but the last was additionally supplemented with 0.5 mg/mL G418 sulfate. An amount of 1×10^4 cells/mL was inoculated into each well of a 96-well plate and incubated overnight at 37 °C in a humidified atmosphere containing 5% CO$_2$. Compounds were dissolved in DMSO and diluted in complete cell culture medium to give a broad range of concentrations such that the final DMSO concentration was not greater than 0.1%. Medium was removed from each well and replaced with compound or control solutions. After 96 h of incubation, the MTT assay was performed to assess chemosensitivity.

Immunocytochemical Analysis of Microtubule Disruption. HT29 cells at 70% confluency were trypsinized and transferred into six-well plates (5×10^5 cells/well) and allowed to adhere overnight at 37 °C in a humidified incubator prior to the treatment, and the immunocytochemical analysis was performed as previously described.[27] In brief, cells were seeded onto sterilized glass coverslips in six-well plates (Corning Glass Works, NY, U.S.). Cells were left to adhere for 24 h. Compound 7 (at 5, 50, and 500 nM) was added to each culture for 24 h. Medium was removed, and the cells were fixed in precooled methanol at −20 °C for 30 min. After washes in PBS, cells were incubated in the primary monoclonal antibody, mouse anti-α-tubulin (Sigma) at a dilution of 1:500 in PBS for 30 min at rt. After washes in PBS, the secondary antibody, TRITC-conjugated rabbit anti-mouse IgG (Dako, Ely, U.K.) was added at a dilution of 1:50 for 30 min. After final washes, the cultures were mounted in Vectashield (Vector Laboratories, Peterborough, U.K.) and stored at 4 °C until analysis. Cells were analyzed and images captured with a Zeiss LSM510 confocal system attached to an Axiovert 200 M inverted microscope using LSM510 software (all from Zeiss, Welwyn Garden City, U.K.).

Induction of ABC Transporter Genes. HT29 and DLD1 cell lines were seeded at 5×10^5 cells/dish and incubated overnight. Cells were treated for 96 h with selected concentrations of colchicine and **7**, respectively. Total RNA was isolated from the cells using RNeasy Mini Kit (QIAGEN) according to the manufacturer's protocol. The RNA concentration and purity were determined using a microvolume spectrophotometer. Reverse transcription was performed using multiscribe reverse transcriptase kit (Applied Biosystems). The ABCB1 and ABCG2 mRNA expression levels were quantified using the Stratagene Mx3005P QPCR system (Agilent Technologies). Quantitative RT-PCR was carried out using TaqMan Universal PCR master mix (Roche Applied Biosystems) and specific primer sets: ABCB1 (5′-CCATAGCTCGTGCCCTTG-3′/5′-AGGGCTTCTTGGACA-ACCTT-3′) and ABCG2 (5′-TTCCACGATATGGATTTACGG-3′/5′-GTTTCCTGTTGCATTGAGTCC-3′). Normalization was performed using PPIA as a human endogenous control (FAM/MGB Probe, Non-Primer Limited, Roche Applied Biosystems). Three independent PCR analyses were performed. Fold induction was expressed as the relative ratio (signal of target)/(signal of PPIA) to the ratio of that in the control in an individual experiment. The significance of results was assessed through a comparison of mean values using a paired two-tailed *t* test with two-way ANOVA followed by Bonferroni correction for multiple testing. Statistical analysis was performed using GraphPad Prism version 4.00 (www.graphpad.com).

■ ASSOCIATED CONTENT

ⓢ Supporting Information

Synthesis details and images of binding models for **1−11**; cell cycle, liver homogenate stability, and chemosensitivity in A459 in the absence/presence of fumitremorgin C for **7**. This material is available free of charge via the Internet at http://pubs.acs.org.

■ AUTHOR INFORMATION

Corresponding Author

*Phone: +44 (0)1274 236482. Fax: +44 (0)1274 233234. E-mail: k.pors1@bradford.ac.uk.

■ ABBREVIATIONS USED

DAPI, 4′,6-diamidino-2-phenylindole; DMEM, Dulbecco's modified Eagle medium; MAP, microtubule-associated protein

■ REFERENCES

(1) Zhao, Y.; Fang, W. S.; Pors, K. Microtubule stabilising agents for cancer chemotherapy. *Expert Opin. Ther. Pat.* **2009**, *19*, 607−622.

(2) Szakacs, G.; Paterson, J. K.; Ludwig, J. A.; Booth-Genthe, C.; Gottesman, M. M. Targeting multidrug resistance in cancer. *Nat. Rev. Drug Discovery* **2006**, *5*, 219−234.

(3) Jordan, M. A.; Wilson, L. Microtubules as a target for anticancer drugs. *Nat. Rev. Cancer* **2004**, *4*, 253−265.

(4) Graening, T.; Schmalz, H. G. Total syntheses of colchicine in comparison: a journey through 50 years of synthetic organic chemistry. *Angew. Chem., Int. Ed.* **2004**, *43*, 3230−3256.

(5) Pasquier, E.; Andre, N.; Braguer, D. Targeting microtubules to inhibit angiogenesis and disrupt tumour vasculature: implications for cancer treatment. *Curr. Cancer Drug Targets* **2007**, *7*, 566−581.

(6) Shi, Q.; Chen, K.; Morris-Natschke, S. L.; Lee, K. H. Recent progress in the development of tubulin inhibitors as antimitotic antitumor agents. *Curr. Pharm. Des.* **1998**, *4*, 219−248.

(7) Gelmi, M. L.; Mottadelli, S.; Pocar, D.; Riva, A.; Bombardelli, E.; De Vincenzo, R.; Scambia, G. N-Deacetyl-N-aminoacylthiocolchicine derivatives: synthesis and biological evaluation on MDR-positive and MDR-negative human cancer cell lines. *J. Med. Chem.* **1999**, *42*, 5272−5276.

(8) Tang-Wai, D. F.; Brossi, A.; Arnold, L. D.; Gros, P. The nitrogen of the acetamido group of colchicine modulates P-glycoprotein-mediated multidrug resistance. *Biochemistry* **1993**, *32*, 6470−6476.

(9) Ringel, I.; Jaffe, D.; Alerhand, S.; Boye, O.; Muzaffar, A.; Brossi, A. Fluorinated colchicinoids: antitubulin and cytotoxic properties. *J. Med. Chem.* **1991**, *34*, 3334−3338.

(10) Atkinson, J. M.; Falconer, R. A.; Edwards, D. R.; Pennington, C. J.; Siller, C. S.; Shnyder, S. D.; Bibby, M. C.; Patterson, L. H.; Loadman, P. M.; Gill, J. H. Development of a novel tumor-targeted vascular disrupting agent activated by membrane-type matrix metalloproteinases. *Cancer Res.* **2010**, *70*, 6902−6912.

(11) Buey, R. M.; Calvo, E.; Barasoain, I.; Pineda, O.; Edler, M. C.; Matesanz, R.; Cerezo, G.; Van-derwal, C. D.; Day, B. W.; Sorensen, E. J.; Lopez, J. A.; Andreu, J. M.; Hamel, E.; Diaz, J. F. Cyclostreptin binds covalently to microtubule pores and lumenal taxoid binding sites. *Nat. Chem. Biol.* **2007**, *3*, 117−125.

(12) Field, J. J.; Pera, B.; Calvo, E.; Canales, A.; Zurwerra, D.; Trigili, C.; Rodriguez-Salarichs, J.; Matesanz, R.; Kanakkanthara, A.; Wakefield, S. J.; Singh, A. J.; Jimenez-Barbero, J.; Miller, J. H.; Lopez, J. A.; Hamel, E.; Barasoain, I.; Altmann, K. H.; Diaz, J. F. Zampanolide, a potent new microtubule-stabilizing agent, covalently reacts with the taxane luminal site in tubulin alpha,beta-heterodimers and microtubules. *Chem. Biol.* **2012**, *19*, 686−698.

(13) Bagnato, J. D.; Eilers, A. L.; Horton, R. A.; Grissom, C. B. Synthesis and characterization of a cobalamin−colchicine conjugate as a novel tumor-targeted cytotoxin. *J. Org. Chem.* **2004**, *69*, 8987−8996.

(14) Ravelli, R. B.; Gigant, B.; Curmi, P. A.; Lachkar, S.; Sobel, A.; Knossow, M. Insight into tubulin regulation from a complex with colchicine and a stathmin-like domain. *Nature* **2004**, *428*, 198−202.

(15) Das, L.; Datta, A. B.; Gupta, S.; Poddar, A.; Sengupta, S.; Janik, M. E.; Bhattacharyya, B. -NH-dansyl isocolchicine exhibits a significantly improved tubulin-binding affinity and microtubule inhibition in comparison to isocolchicine by binding tubulin through its A and B rings. *Biochemistry* **2005**, *44*, 3249−3258.

(16) Barron, D. M.; Chatterjee, S.; Ravindra, R.; Roof, R.; Baloglu, E.; Kingston, D. G.; Bane, S. A fluorescence-based high-throughput assay for antimicrotubule drugs. *Anal. Biochem.* **2003**, *315*, 49−56.

(17) Tateishi, T.; Soucek, P.; Caraco, Y.; Guengerich, F. P.; Wood, A. J. Colchicine biotransformation by human liver microsomes. Identification of CYP3A4 as the major isoform responsible for colchicine demethylation. *Biochem. Pharmacol.* **1997**, *53*, 111−116.

(18) Dvorak, Z.; Modriansky, M.; Pichard-Garcia, L.; Balaguer, P.; Vilarem, M. J.; Ulrichova, J.; Maurel, P.; Pascussi, J. M. Colchicine down-regulates cytochrome P450 2B6, 2C8, 2C9, and 3A4 in human hepatocytes by affecting their glucocorticoid receptor-mediated regulation. *Mol. Pharmacol.* **2003**, *64*, 160−169.

(19) Deeken, J. F.; Robey, R. W.; Shukla, S.; Steadman, K.; Chakraborty, A. R.; Poonkuzhali, B.; Schuetz, E. G.; Holbeck, S.; Ambudkar, S. V.; Bates, S. E. Identification of compounds that correlate with ABCG2 transporter function in the National Cancer Institute Anticancer Drug Screen. *Mol. Pharmacol.* **2009**, *76*, 946−956.

(20) Stengel, C.; Newman, S. P.; Leese, M. P.; Potter, B.; Reed, M. J.; Purohit, A. Class III beta-tubulin expression and in vitro resistance to microtubule targeting agents. *Br. J. Cancer* **2010**, *102*, 316−324.

(21) Joe, P. A.; Banerjee, A.; Luduena, R. F. The roles of cys124 and ser239 in the functional properties of human betaIII tubulin. *Cell Motil. Cytoskeleton* **2008**, *65*, 476−486.

(22) Risinger, A. L.; Jackson, E. M.; Polin, L. A.; Helms, G. L.; LeBoeuf, D.; Joe, P.; Luduena, R. F.; Kruh, G. D.; Mooberry, S. L. The taccalonolides: microtubule stabilizers that circumvent clinically relevant taxane resistance mechanisms. *Cancer Res.* **2008**, *68*, 8881−8888.

(23) Jackson, J. R.; Patrick, D. R.; Dar, M. M.; Huang, P. S. Targeted anti-mitotic therapies: Can we improve on tubulin agents? *Nat. Rev. Cancer* **2007**, *7*, 107−117.

(24) Pors, K.; Loadman, P. M.; Shnyder, S. D.; Sutherland, M.; Sheldrake, H. M.; Guino, M.; Kiakos, K.; Hartley, J. A.; Searcey, M.; Patterson, L. H. Modification of the duocarmycin pharmacophore enables CYP1A1 targeting for biological activity. *Chem. Commun. (Cambridge, U. K.)* **2011**, *47*, 12062−12064.

(25) Pors, K.; Shnyder, S. D.; Teesdale-Spittle, P. H.; Hartley, J. A.; Zloh, M.; Searcey, M.; Patterson, L. H. Synthesis of DNA-directed pyrrolidinyl and piperidinyl confined alkylating chloroalkylaminoanthraquinones: potential for development of tumor-selective N-oxides. *J. Med. Chem.* **2006**, *49*, 7013−7023.

(26) Williams, R. C., Jr.; Lee, J. C. Preparation of tubulin from brain. *Methods Enzymol.* **1982**, *85* (Part B), 376−385.

(27) Shnyder, S. D.; Cooper, P. A.; Millington, N. J.; Pettit, G. R.; Bibby, M. C. Auristatin PYE, a novel synthetic derivative of dolastatin 10, is highly effective in human colon tumour models. *Int. J. Oncol.* **2007**, *31*, 353−360.